A Technique for Estimating the State of Health of Lithium Batteries Through a Dual-Sliding-Mode Observer

IL-Song Kim, *Member, IEEE*

***Abstract*—A new state-of-health (SOH) estimation method for lithium batteries that uses a dual-sliding-mode observer is presented. The capacity fade and resistance deterioration were estimated by the dual-sliding-mode observer. The dual-sliding-mode observer consists of a fast-paced time-varying observer and a slow-paced time-varying observer. The fast-paced time-varying observer estimates parameters, such as the state of charge and terminal voltage, and polarization effects. The slow-paced time-varying observer estimates the SOH in terms of the capacity fade and resistance deterioration. The convergence of the proposed observer was proved by the Lyapunov equation. The structure of the proposed system is simple and easy to implement and shows robust control properties against modeling errors and temperature variations. The test results show that the proposed observer system has superior tracking performance than previous ampere-counting method.**

***Index Terms*—Capacity fade, dual-sliding-mode observer, lithium battery, resistance deterioration, state of health (SOH).**

NOMENCLATURE

C_n	Nominal capacity of the cell [A·h].
$\hat{C}_n$	Estimated nominal capacity [A·h].
C_p	Polarization capacitance [F].
e_y, e_p, e_z	Error states for the SOC observer.
e_{zh}, e_c, e_{ht}, e_R	Error states for the SOH observer.
h_1, h_2, h_3, h_4	Positive observer feedback gain for parametric estimation.
L_1, L_2, L_3	Positive observer feedback gain for SOC estimation.
R_p	Diffusion resistor [Ω].
R_t	Ohmic resistance [Ω].
$\hat{R}_t$	Estimated ohmic resistance [Ω].
V_p	Polarization voltage [V].
$\hat{V}_p$	Estimated polarization voltage [V].
V_t	Cell terminal voltage [V].
$\hat{V}_t$	Estimated cell terminal voltage [V].
$V_{\rm oc}(Z)$	Open-circuit voltage as a function of the SOC Z.
Z	State of charge.
$\hat{Z}$	Estimated SOC.
Z_h	Filtered SOC.
$\hat{Z}_h$	Estimated filtered SOC.
α	Capacity degradation factor.
β	Resistance degradation factor.
$\Delta f_1, \Delta f_2, \Delta f_3$	Errors in modeling for the SOC estimation.
$\Delta f_z, \Delta f_c, \Delta f_V, \Delta f_R$	Errors in modeling for the parametric estimation.
θ	Time-varying system parameter.

Manuscript received April 9, 2009; revised August 29, 2009 and October 13, 2009. Current version published April 14, 2010. Recommended for publication by Associate Editor J. A. Pomilio.

The author is with the Department of Electrical Engineering, Chung-Ju National University, Chung-Ju 380-702, Korea (e-mail: iskim@cjnu.ac.kr).

Color versions of one or more of the figures in this paper are available online at http://ieeexplore.ieee.org.

Digital Object Identifier 10.1109/TPEL.2009.2034966

I. INTRODUCTION

LITHIUM-ION or lithium-polymer batteries (Li-PBs) are widely used in mobile equipment, electric vehicles, and space and aircraft power systems for their lightness of weight, high energy density, high galvanic potential, and long lifetimes, in comparison with lead–acid or nickel–metal hydride batteries.

Due to the complex chemical and physical processes of batteries, the behavior of batteries shows nonlinear characteristics, and therefore, is hard to predict in comparison with the behavior of electrical and mechanical devices. This behavior depends upon the charge/discharge current, temperature variation, state of charge (SOC), state of health (SOH), hysteresis level, and the prior status of the battery. The behavior can be better understood through the modeling of the physical parameters. The main parameters that characterize battery behavior are the SOC, internal resistance, capacity, polarization capacitance, polarization resistance, and self-discharge resistance. Among these elements, the key parameters will be the SOC and SOH of the battery. In terms of modeling the properties, the SOC and SOH are closely related parameters. The variable of the SOH can be considered as time-varying parameters in the SOC calculation. The SOC corresponds to the stored charge that is available for doing work, relative to that which is available after the battery has been fully charged. Since the battery charge/discharge current control is based on the SOC information, the correct indication of the SOC is of considerable importance for application in mobile communication and hybrid electric vehicles (HEVs).

The other key parameter is the SOH. SOH is defined as the ability of a cell to store energy, source and sink high currents, and retain charge over extended periods, relative to its initial or nominal capabilities. The available charge that is stored within a fully charged cell is expected to fall with cell usage, as active material on the cell plates gradually degrades by mechanisms such as: the loss of the plate active surface area due to repeated dissolution and recrystallization, the loss of electrical contact

between metallic grids and active materials, and the growth of large inactive materials.

Many studies have been performed to indicate the SOH status [1]–[7]. Most of them are based on chemical analysis of the battery. The drawback of these methods is that they are hard to apply to electrical circuits. As in the case of the SOC, the SOH is hard to measure with respect to electrical circuits; therefore, it should be estimated through a mathematical algorithm. Several papers that are based upon mathematical modeling have been presented and most of them use impedance measurement and the Kalman filter method [8]–[11]. The impedance measurement method shows good accuracy; however, it cannot be used in online applications. It should be measured with stand-alone battery, which is disconnected to the charger or load.

This is a critical limitation in mobile or transportation applications, such as HEVs or photovoltaic power generation systems. The Kalman filter method also has some limitations in real applications. The operating environment should be in the zero-mean noise condition and the computational burden is high due to complex matrix operations.

In this paper, a new dual-sliding-mode-observer design method has been proposed for the estimation of the SOH of lithium batteries. The proposed method is a model-based approach. Heuristic experimental data are used in conventional methods; however, the proposed methods are based on a mathematical model to derive a unified solution for the SOC and SOH. The proposed dual-sliding-mode observer can overcome the aforementioned drawbacks by using sliding-mode techniques.

This paper consists of six sections. In Section II, a simple electrical-battery modeling technique is presented to describe the battery charge/discharge characteristics. In Section III, the sliding-mode-observer design methodology for estimating the SOC is presented. The dual-sliding-mode observer for estimating the SOH is presented in the Section IV. In Sections V and VI, the results of the cell characterization test and the dual-sliding-mode observer are shown to verify the performance of the proposed system.

II. Battery Modeling

There have been many attempts to develop battery models. The most common models are the electrochemistry model and the electrocircuit model. While detailed chemistry-based models have been built to investigate the internal dynamics of batteries, these models are generally not suitable for the design of electrical systems [12]. On the other hand, circuit-based models have been built in terms of electric-circuit parameters, such as capacitances, resistances, voltage sources, etc. Circuit-based models are a commonly used method for battery controllers because it is possible to represent in terms of mathematical formulas. It has been known that perfect battery modeling is hard to achieve for every operating condition, even through the electrocircuit model. Therefore, many complicated electrical modeling methods have been developed to reduce modeling errors. However, these methods increase the computational time, system complexity, and requirement for resources; moreover, they can be a cause of instability.

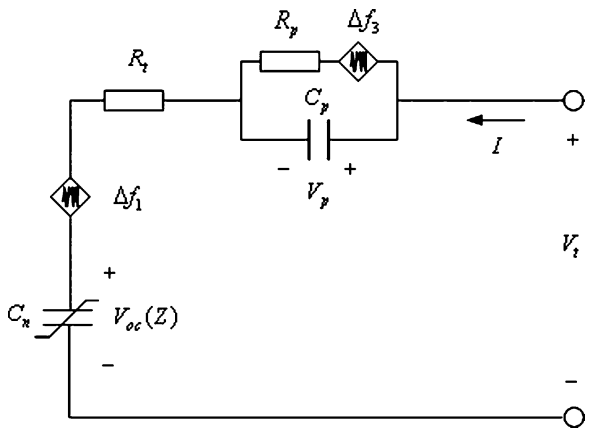

Fig. 1. RC electrical model of a lithium battery.

A simple RC model is employed for lithium-battery modeling in this paper. All of the modeling errors, uncertainties, and time-varying elements are considered as external disturbances. The merits of this model are that it is simple and entails little computational time; further, the modeling errors are compensated for by the robust sliding-mode observer.

A RC electrical model of the Li-PB consists of: an open-circuit voltage (OCV), which is denoted by $V_{\rm oc}(Z)$ and is a function of the SOC Z, a capacitor C_p to model the polarization effect, a diffusion resistance R_p as a function of the current I, an ohmic resistance R_t, and the terminal voltage V_t. The RC electrical modeling including uncertainties is shown in Fig. 1. The symbols Δf_1 and Δf_3 represent modeling errors. The terminal voltage is given as follows:

$$V_t = V_{\rm oc}(Z) + IR_t + V_p + \Delta_{\rm unknown}. \tag{1}$$

The SOC can be defined as the ratio of the remaining capacity to the nominal capacity of the cell, where the remaining capacity is the number of ampere·hours that can be drawn from the cell at room temperature at the C/30 rate before the cell is fully discharged. However, in real operating conditions, the value of the capacity is changed by the temperature, the level of the SOC Z, and aging factors. The capacity can be divided into a nominal term and a nonlinear term. The nominal value is a constant and can be known by the charge–discharge cycle test data. The nonlinear term represents the capacitance deviation, temperature effect, and unknown term; thus, it cannot be measured. Therefore, based on this definition, the mathematical relationship for the SOC is developed as

$$\begin{aligned} Z(t) &= Z(0) + \int_0^t \frac{I(\tau)}{C_{\rm capacity}}\, d\tau \\ &= Z(0) + \int_0^t \frac{I(\tau)}{C_n}\, d\tau + \int_0^t \frac{I(\tau)}{C_{\rm nonlinear}}\, d\tau \end{aligned} \tag{2}$$

where $Z(t)$ is the SOC, C_n is the nominal capacity of the cell, and $C_{\rm nonlinear}$ is the nonlinear term for which the maximum

bound is limited. The time derivative for the SOC Z can be expressed as follows:

$$\dot{Z} = \frac{I}{C_n} + \Delta f_2 \tag{3}$$

where I is the instantaneous current, which is positive for charging and negative for discharging.

By substituting (1) into (3), one obtains

$$\begin{aligned}\dot{Z} &= \frac{1}{R_t C_n}(V_t - V_{\rm oc}(Z) - V_p) + \Delta f_2 \\ &= a_2 V_t - a_2 V_{\rm oc}(Z) - a_2 V_p + \Delta f_2 \end{aligned} \tag{4}$$

where $a_2 = 1/R_t C_n$ and Δf_2 is the uncertainty caused by unknown nonlinear capacity term.

The polarization voltage due to the current is shown as

$$\dot{V}_p = -\frac{1}{R_p C_p} V_p + \frac{I}{C_p} + \frac{I}{\Delta C_p} = -a_1 V_p + b_2 I + \Delta f_3 \tag{5}$$

where $a_1 = 1/R_p C_p$, $b_2 = 1/C_p$, and Δf_3 is the uncertainty caused by unknown nonlinear polarization voltage term.

Due to the high capacitance, the derivative of the terminal voltage with respect to the current is negligible if a fast sampling time is obtained (i.e., $(\Delta V_t/\Delta I) \approx 0$). Therefore, the derivative of the second term in (1) can be considered as zero, and the complete state equation from (1), (4), and (5) is

$$\begin{aligned}\dot{V}_t &= V_{\rm oc}(\dot{Z}) + \frac{d}{dt}(IR_t) + \dot{V}_p = \frac{I}{C_n} - \frac{V_p}{R_p C_p} + \frac{I}{C_p} \\ &= \frac{I}{C_n} - \frac{1}{R_p C_p}(V_t - V_{\rm oc}(Z) - IR_t) + \frac{I}{C_p} \\ &= -a_1 V_t + a_1 V_{\rm oc}(Z) + b_1 I + \Delta f_1 \end{aligned} \tag{6}$$

where $b_1 = ((1/C_n) + (1/C_p) + (R_t/R_p C_p))$, and Δf_1 is the uncertainty caused by unknown nonlinear terminal voltage term.

III. Sliding-Mode-Observer Design for SOC Estimation

Since the observability matrix of the system always has full rank, the internal state of the battery can be estimated by the observer [13]–[15]. The output equation of the sliding-mode observer is given by

$$\dot{\hat{V}}_t = -a_1 \hat{V}_t + a_1 V_{\rm oc}(\hat{Z}) + b_1 I + L_1 {\rm sgn}(V_t - \hat{V}_t) \tag{7}$$

where $(\hat{V}_t, \hat{Z})$ are the estimates for (V_t, Z) and $L_1$is a constant positive-feedback gain.

When the error is defined as $e_y = V_t - \hat{V}_t$, the following error equation is obtained:

$$\dot{e}_y = -a_1 e_y + a_1(V_{\rm oc}(Z) - V_{\rm oc}(\hat{Z})) + \Delta f_1 - L_1 {\rm sgn}(e_y) \tag{8}$$

where

$$ {\rm sgn}(e_y) = \begin{cases} +1, e_y > 0 \\ -1, e_y < 0. \end{cases}$$

The convergence of the error equation can be proved through the Lyapunov candidate function by setting $V_y = 1/2 e_y^2$. The following relationship is obtained from (8) to satisfy the convergence condition:

$$L_1 > |\Delta f_1 + a_1(V_{\rm oc}(Z) - V_{\rm oc}(\hat{Z})|. \tag{9}$$

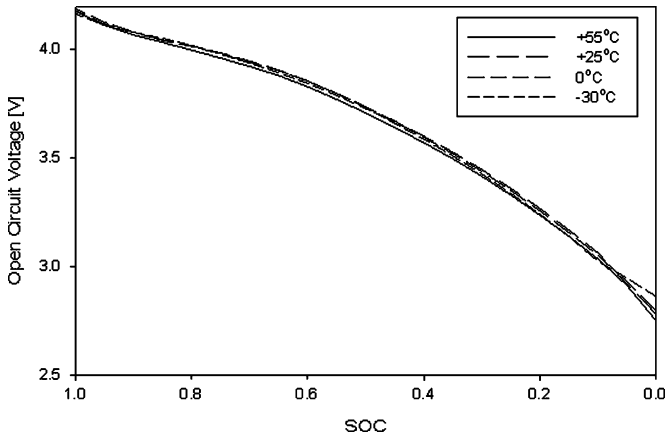

Fig. 2. OCV versus SOC of a Li-PB.

The range of $V_{\rm oc}(Z)$ is from 2.8 to 4.2 V, as can be seen in Fig. 2. Therefore, $V_{\rm oc}(\hat{Z})$ also has same range.

The constant a_1 is obtained from the experimental result as

$$a_1 = \frac{1}{R_p C_p} = \frac{1}{1.5 \times 200} = 0.003. \tag{10}$$

Therefore, we can assume the maximum error bound for $|a_1(V_{\rm oc}(Z) - V_{\rm oc}(\hat{Z})|$ as being

$$\approx 0.003 \times 1.4 \approx 0.0042.$$

This value may have some small error due to the nonlinear characteristics of C_P and R_p.

Then, we may deduce

$$\begin{aligned} L_1 &> |\Delta f_1 + a_1(V_{\rm oc}(Z) - V_{\rm oc}(\hat{Z})| \approx |\Delta f_1 + 0.0042| \\ &> |\Delta f_1| + 0.0042. \end{aligned} \tag{11}$$

Select $L_1 > |\Delta f_1| + 0.0042$. Then, the sign of $\dot{e}_y$ is negative (positive) if e_y is positive (negative), regardless of the difference $V_{\rm oc}(Z) - V_{\rm oc}(\hat{Z})$. Therefore, $\dot{V}_y = e_y \dot{e}_y < 0$. After some finite time, $\dot{e}_y = 0$ and $e_y = 0$ for all subsequent time points.

According to the equivalent control method, the error system in the sliding mode behaves as if $L_1 {\rm sgn}(e_y)$ is replaced by its equivalent value $(L_1 {\rm sgn}(e_y))_{\rm eq}$, which can be calculated from (8) assuming $\dot{e}_y = 0$ and $e_y = 0$. Once the sliding surface is reached, then from the equivalent control concept, e_y and $\dot{e}_y$ reduce to zero and the uncertaintyΔf_1 vanishes. Then, the resulting equation from (8) can be written as follows:

$$V_{\rm oc}(Z) - V_{\rm oc}(\hat{Z}) = \left\{ \frac{L_1}{a_1} {\rm sgn}(e_y) \right\}_{\rm eq}. \tag{12}$$

The next observer equation for Z is obtained as

$$\dot{\hat{Z}} = a_2 \hat{V}_t - a_2 V_{\rm oc}(\hat{Z}) - a_2 \hat{V}_p + L_2 {\rm sgn}(Z - \hat{Z}) \tag{13}$$

where $(\hat{Z}, \hat{V}_p)$ are the estimates for (Z, V_p) and L_2 is a constant positive-feedback gain.

Define the errors as $e_Z = Z - \hat{Z}$ and $e_p = V_p - \hat{V}_p$; then, the following error equation is obtained:

$$\dot{e}_Z = a_2 e_y - a_2(V_{\rm oc}(Z) - V_{\rm oc}(\hat{Z})) - a_2 e_p + \Delta f_2 - L_2 \mathrm{sgn}(e_Z). \quad (14)$$

As OCV is monotonically increasing with respect to the SOC Z, $V_{\rm oc}(Z) - V_{\rm oc}(\hat{Z})$ can be considered as being piecewise linear in$(Z - \hat{Z})$. Therefore

$$V_{\rm oc}(Z) - V_{\rm oc}(\hat{Z}) \approx k(Z - \hat{Z}). \quad (15)$$

The error system for Z is given by

$$\dot{e}_Z = a_2 e_y - a_2 k e_Z - a_2 e_p + \Delta f_2 - L_2 \mathrm{sgn}(e_Z) \quad (16)$$

where k is a piecewise linear gain and the maximum value is determined from the experimental data.

Choose a Lyapunov candidate function $V_Z = 1/2 e_Z^2$. Select $L_2 > |\Delta f_2|$; $\dot{e}_Z$ and e_Z have opposite signs. Therefore, $\dot{V}_Z = e_Z \dot{e}_Z < 0$ and, as in the previous case, $\dot{e}_Z = 0$ and $e_Z = 0$ for all subsequent time points. Then, the following relationship is obtained:

$$e_p = \left\{ \frac{-L_2}{a_2} \mathrm{sgn}(e_Z) \right\}_{\rm eq} = \left[\frac{-L_2}{a_2} \mathrm{sgn} \left(\left\{ \frac{L_1}{a_1 k} \mathrm{sgn}(e_y) \right\}_{\rm eq} \right) \right]_{\rm eq}. \quad (17)$$

Finally, the observer for V_p is built as

$$\dot{\hat{V}}_p = -a_1 \hat{V}_p + b_2 I + L_3 \mathrm{sgn}(V_p - \hat{V}_p). \quad (18)$$

The error system is

$$\dot{e}_p = -a_1 e_p + \Delta f_3 - L_3 \mathrm{sgn}(e_p). \quad (19)$$

As in the previous case, select $L_3 > |\Delta f_3|$. Then, the error e_p goes to zero if L_3 is larger than the uncertainties. The resulting observer equations are as follows:

$$\begin{aligned} \dot{\hat{V}}_t &= -a_1 \hat{V}_t + a_1 V_{\rm oc}(\hat{Z}) + b_1 I + L_1 \mathrm{sgn}(V_t - \hat{V}_t) \\ \dot{\hat{Z}} &= a_2 \hat{V}_t - a_2 V_{\rm oc}(\hat{Z}) - a_2 \hat{V}_p + L_2 \mathrm{sgn} \left(\left\{ \frac{L_1}{a_1 k} \mathrm{sgn}(e_y) \right\}_{\rm eq} \right) \\ \dot{\hat{V}}_p &= -a_1 \hat{V}_p + b_2 I + L_3 \mathrm{sgn} \left(\left[\frac{-L_2}{a_2} \mathrm{sgn} \left(\left\{ \frac{L_1}{a_1 k} \mathrm{sgn}(e_y) \right\}_{\rm eq} \right) \right]_{\rm eq} \right). \end{aligned} \quad (20)$$

The range of the feedback gain should be

$$\begin{aligned} L_1 &> |\Delta f_1| + 0.0042 \\ L_2 &> |\Delta f_2|, \text{ and} \\ L_3 &> |\Delta f_3|. \end{aligned} \quad (21)$$

The boundaries of the uncertainties can be determined by comparing the cell test data with the parameters for modeling.

IV. SOH Estimation Using the Dual-Sliding-Mode Observer

The SOH of batteries can be characterized as power fade and capacity fade (energy fade). The power that a battery can provide is dependent upon the internal resistance. As the resistance increases, the available power is decreased due to the increased *IR* drop. The available energy, which is expressed as watt·hours, is dependent on the capacity. The cell capacity decreases as the cell cycle increases. It is important to be able to estimate these parameters to understand the present battery SOH and predict the remaining service life.

From the SOC estimation results, the entire ranges of the state variables of the RC model can be changed within several minutes. The parameters for modeling may change very slowly, for example, the battery capacity or internal resistance may change by as little as 20% from their initial values in a decade. For modeling purposes, we can conceive of states that change very rapidly and time-varying parameters that change very slowly [16]–[18]. The method for SOC estimation might be modified to concurrently estimate both the state and the slow-paced time-varying parameters by the use of separate sliding-mode observers for state estimation and parametric estimation. The advantage of this method is the ease of observer design and the reduced computational burden due to simple matrix operations.

The state equation in battery modeling is modified to include parametric variations in the following manner:

$$\dot{x} = f(x, u, \theta) + \Delta f$$

and

$$y = C(x, u, \theta) \quad (22)$$

where x is the model state, θ is the set of time-varying model parameters, u is the input, y is the system output, and Δf are the model uncertainties.

Assume there is a true value for θ that describes the cell under consideration. We want to adapt an estimate $\hat{\theta}$ to converge to the true value. The state-space model for parametric dynamics is expressed as

$$\dot{\theta} = f(\theta, u) + \Delta\theta \quad (23)$$

where $\Delta\theta$ is the parametric uncertainty.

Equation (23) states that the parameters are essentially constant, but may change slowly over time by some driving process, which is modeled by the result of the accelerated life cycle test. The output equation for the state-space model of true parametric dynamics is constructed from the battery-model state equation.

Using these two state equations, a standard observer design procedure can be applied to the dual-sliding-mode-observer structure. It consists of two parallel-connected sliding-mode observers. In each sampling time, the state observer and the parameter observer are updated in sequence. First, the state observer is updated through the previous parameter values. Then, the new parameter observer is updated by using new estimates of the state values. The process can be thought

of as essentially comprising two sliding-mode observers running in parallel–one adapting the states and other adapting the parameters—with some information exchange between the observers.

A. Estimating the Capacity Fade C_n

To estimate the cell capacity through the dual-sliding-mode observer, the formula for capacity change can be written as follows:

$$C_n(t) = C_{n0} - \alpha t \tag{24}$$

where C_{n0} is the initial capacity and α is the degradation factor.

Differentiating (24), we obtain

$$\dot{C}_n = -\alpha + \Delta f_C \tag{25}$$

where Δf_C corresponds to the modeling errors that are caused by uncertainties.

From the previous definition of the SOC, the new state variable Z_h is assigned as a filtered output from $\hat{Z}$ and corresponds to the average value of $\hat{Z}$. The definition can be rewritten as

$$\dot{Z}_h = \frac{I}{C_n} + \Delta f_Z. \tag{26}$$

In (26), Z_h is considered as the output of a parametric estimator. As in the previous section, the output observer equation is expressed as

$$\dot{\hat{Z}}_h = \frac{I}{\hat{C}_n} + h_1 \mathrm{sgn}(Z_h - \hat{Z}_h) \tag{27}$$

where $(\hat{Z}_h, \hat{C}_n)$ are the estimates for (Z_h, C_n) and $h_1$is a constant positive-feedback gain.

Define the errors as $e_{Zh} = Z_h - \hat{Z}_h$ and $e_C = C_n - \hat{C}_n$. Then, the following error equation is obtained:

$$\dot{e}_{Zh} = I\left(\frac{1}{C_n} - \frac{1}{\hat{C}_n}\right) + \Delta f_Z - h_1 \mathrm{sgn}(e_{Zh}). \tag{28}$$

Choose the Lyapunov candidate function $V_{Zh} = 1/2e_{Zh}^2$. C_n has a positive value, whose range is 0–21000 F. As $C_n(t)$ is monotonically decreasing in t, the estimation error $((1/C_n) - (1/\hat{C}_n))$ has a small finite value. The condition for convergence of the error equation is

$$\begin{aligned} h_1 &> \left|\Delta f_z + I\left(\frac{1}{C_n} - \frac{1}{\hat{C}_n}\right)\right| \\ &> |\Delta f_z| + \left|I\left(\frac{1}{C_n} - \frac{1}{\hat{C}_n}\right)\right| \\ &> |\Delta f_z| + \Delta_0. \end{aligned} \tag{29}$$

The exact range of Δ_0 is hard to calculate; however, it has a relatively smaller value than that of Δf_z. Equation (29) can be rewritten as

$$\begin{aligned} h_1 &> |\Delta f_z| + \Delta_0 \\ &\gg |\Delta f_z|. \end{aligned} \tag{30}$$

Select $h_1 \gg |\Delta f_Z|$; the signs of $\dot{e}_{Zh}$ and e_{Zh} are opposing. Therefore, $\dot{V}_{Zh} = e_{Zh}\dot{e}_{Zh} < 0$. As in the previous case, $\dot{e}_{Zh} = 0$ and $e_{Zh} = 0$ for all subsequent time points.

By the equivalent control concept, we have

$$\left(\frac{1}{C_n} - \frac{1}{\hat{C}_n}\right) = \frac{h_1}{I}\mathrm{sgn}(e_{Zh}). \tag{31}$$

Therefore

$$\begin{aligned} \mathrm{sgn}(C_n - \hat{C}_n) &= -\mathrm{sgn}\left(\frac{1}{C_n} - \frac{1}{\hat{C}_n}\right) \\ &= \mathrm{sgn}\left\{-\frac{h_1}{I}\mathrm{sgn}(e_{Zh})\right\}_{\mathrm{eq}}. \end{aligned} \tag{32}$$

This holds as long as the estimate $\hat{C}_n$ remains positive.

In similar manner, the observer equation for C_n can be derived as

$$\dot{\hat{C}}_n = -\alpha + h_2 \mathrm{sgn}(C_n - \hat{C}_n). \tag{33}$$

The error equation for C_n is given by

$$\dot{e}_C = \Delta f_c - h_2 \mathrm{sgn}(e_C). \tag{34}$$

Select $h_2 > |\Delta f_c|$; the signs of $\dot{e}_c$ and e_c are opposing. Therefore, e_C converges to zero. The resulting observer equations for capacity estimation are

$$\dot{\hat{Z}}_h = \frac{I}{\hat{C}_n} + h_1 \mathrm{sgn}(e_{Zh})$$

and

$$\dot{\hat{C}}_n = -\alpha + h_2 \mathrm{sgn}\left\{-\frac{h_1}{I}\mathrm{sgn}(e_{Zh})\right\}_{\mathrm{eq}}. \tag{35}$$

B. Estimating the Resistance R_t

To estimate the cell resistance through a sliding-mode observer, the cell output equation can be written as

$$\begin{aligned} \dot{V}_{ht} &= -a_1 V_{ht} + a_1 V_{\mathrm{oc}}(Z_h) + b_1 I + \Delta f_V \\ &= -a_1 V_{ht} + a_1 V_{\mathrm{oc}}(Z_h) + \left(\frac{1}{C_n} + R_t a_1 + b_2\right) I + \Delta f_V. \end{aligned} \tag{36}$$

The cell output voltage is denoted as V_{ht} to distinguish it from the state-estimator output voltage V_t. Assume C_n, Z_h are parameters that are updated through the parametric estimator; thus, they can be considered as known parameters. The resistance R_t is considered as a time-varying parameter that is to be estimated by the sliding observer. Then, the output observer equation for the cell voltage is given as

$$\begin{aligned} \dot{\hat{V}}_{ht} = &-a_1 \hat{V}_{ht} + a_1 V_{\mathrm{oc}}(Z_h) + \left(\frac{1}{C_n} + \hat{R}_t a_1 + b_2\right) I \\ &+ h_3 \mathrm{sgn}(V_{ht} - \hat{V}_{ht}). \end{aligned} \tag{37}$$

Let $e_{hy} = V_{ht} - \hat{V}_{ht}$, and $e_R = R_t - \hat{R}_t$. Then,

$$\dot{e}_{hy} = -a_1 e_{hy} + e_R a_1 I + \Delta f_V - h_3 \mathrm{sgn}(e_{hy}). \tag{38}$$

As in the previous case, if $h_3 \gg |\Delta f_v|$, $e_{hy} \approx 0$ via the Lyapunov inequality equation.

By the equivalent control concept

$$e_R = \left\{ \frac{h_3}{a_1 I} \mathrm{sgn}(e_{hy}) \right\}_{\mathrm{eq}}. \tag{39}$$

The cell resistance R_t is a slow-paced time-varying value, which increases with the cycling time. Its behavior can be described as

$$R_t = R_{t0} + \beta t \tag{40}$$

where R_{t0} is the initial resistance and β is a degradation factor.

The differentiation of (40) yields

$$\dot{R}_t = \beta + \Delta f_R \tag{41}$$

where Δf_R is an error that is caused by uncertainties.

In a similar manner, the observer equation for R_t is

$$\dot{\hat{R}}_t = \beta + h_4 \ \mathrm{sgn}(R_t - \hat{R}_t) = \beta + h_4 \ \mathrm{sgn}(e_R). \tag{42}$$

The error equation for R_t is given by

$$\dot{e}_R = \Delta f_R - h_4 \ \mathrm{sgn}(e_R). \tag{43}$$

Therefore, $e_R \approx 0$ if $h_4 > |\Delta f_R|$.

The resistance can be estimated in the same manner as the capacity.

V. Cell Parameter Extraction

A large-sized Li-PB was used for the test. The cell comprises an $LiMn_2O_4$ cathode and an artificial graphite anode and is designed for high-power application. It has a nominal capacity of 6.0 A·h and a nominal voltage of 3.8 V.

Cell characterization tests were performed to extract cell parameters. The parameters are based on nominal data, which are obtained from the test result for a temperature of 25 °C. The errors in modeling and values of uncertainties are obtained from the boundaries of the operating temperature, which ranges from −30 to 55 °C. This method can be applied to other kinds of battery by changing the nominal parameters.

The RC model parameters are obtained from the cell characterization test data. The nominal capacity C_n is determined from the cycling test, wherein the cell is discharged from the full-charge voltage to the cut-off voltage at the rated current. The polarization capacitance relies on a high-frequency excitation test, which executes 10-C discharge pulses at intervals of 500 ms to determine the time constant that is given by C_p and the associated resistance R_p. The detailed diagram to determine the cell parameters is shown in Fig. 3. Actually, the cell parameters are not constant, but vary with the SOC. The nominal values are chosen for the parameters for a simple RC model. The resulting values are: $C_n = 6$ A·h, $C_p = 200$ F, and $R_t = 0.003\ \Omega$. R_p is a nonlinear resistance that varies between 4 mΩ and 1.5 Ω, depending on the current flow. The circuit parameters are obtained by these numbers.

A periodic discharge test was performed to verify the parameters for modeling. The results are shown in Fig. 4. As can be seen in the figure, the shapes of the true cell response and the RC model output are similar in general. The errors in modeling are quite large for finite periods; however, these errors can be overcome by sliding-mode control actions.

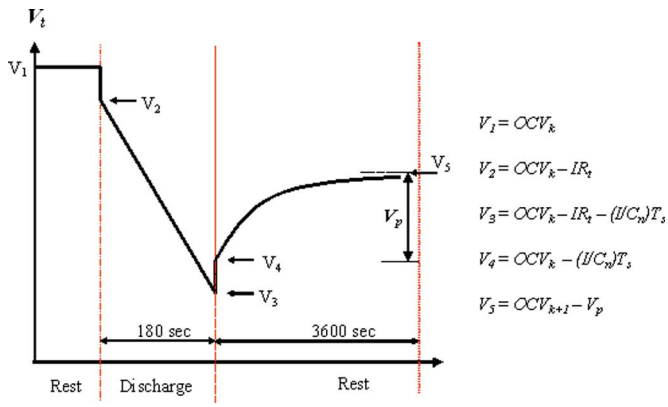

Fig. 3. Cell parameter extraction diagram.

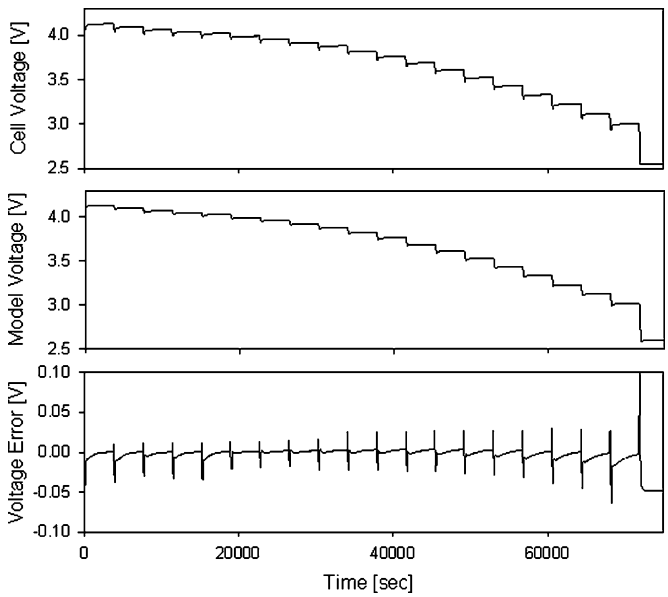

Fig. 4. Result on cell modeling for the discharge test.

The second test was to identify the modeling errors that are caused by temperature variations. The chamber temperature was set to the lower limit of −30 °C, nominal level of 25 °C, and upper limit of 55 °C. The preceding test was performed at each temperature. Then, each state error was calculated from the measured V_t and the true SOC of the cycler. The polarization voltage error is not directly measured. Instead, it can be inferred from the terminal voltage waveform when the discharge current is changed to zero. The errors in modeling for each state variable that are caused by temperature variations are shown in Fig. 5.

VI. Experimental Result for SOC and SOH Estimations

The overall observer system, including test equipment, is shown in Fig. 6. The cell model parameters are obtained from

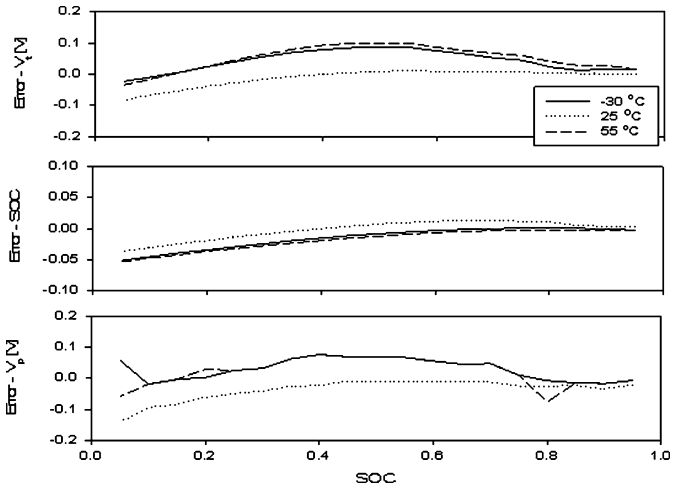

Fig. 5. Errors in modeling for temperature variations.

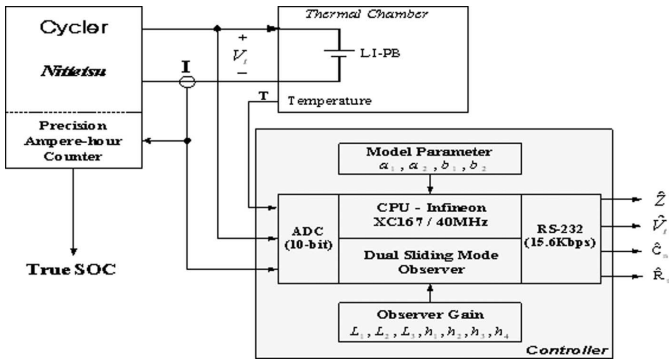

Fig. 6. Configuration of the proposed observer system.

cell characterization test results and the sliding-mode-observer equations are established online for the charge/discharge current of the Li-PB, as can be seen in Fig. 6. The input parameters for the observer system are the charge/discharge current, terminal voltage, and temperature of the cell. The charge/discharge current is simultaneously applied to the Li-PB and sliding-mode observer. The terminal voltage of the Li-PB is considered as the output of the system and fed into the sliding-mode observer to complete the observer equation. The outputs of the observer are the estimated SOC, SOH, and terminal voltage. The purpose of the estimated terminal voltage is to verify the correct operation of the observer through the sliding-mode action.

The controller has been built with an Infineon 16-bit microprocessor XC167–40 [in megahertz]. It contains an internal 10-bit A/D converter with a very fast conversion speed. The computing time for one cell, including the current and voltage measurement, is around 10 ms. Conventional methods for Kalman filters may entail 50 ms due to complex matrix calculations.

The block diagram of the dual-sliding-mode observer for SOC and SOH estimations is shown in Fig. 7. The SOC and SOH observers are operated in parallel and the estimated parameters and state variables are exchanged between observers for each sampling time point. The SOC observer generates the

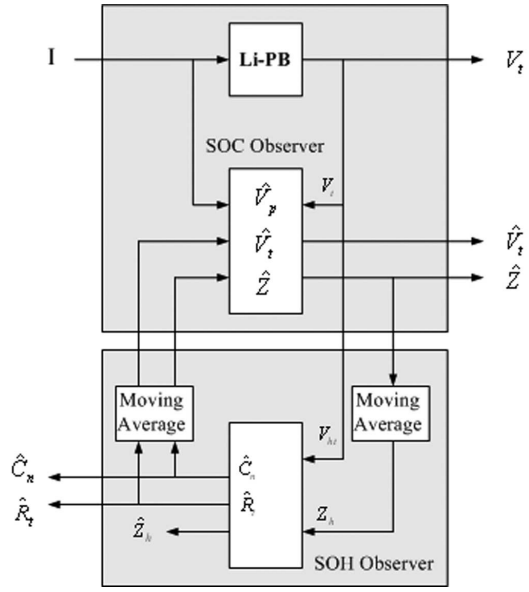

Fig. 7. Dual-sliding-mode observer for SOC and SOH estimations.

TABLE I
GAIN LIST

Variable	L1	L2	L3	h1	h2	h3	h4
Value	0.01	0.2	0.1	0.1	10	0.001	0.000001

estimated SOC $\hat{Z}$ using the previous parametric values and the current input states. Since the estimated SOC $\hat{Z}$ has a chattering value, it should be averaged to be used as input in the parametric-estimation observer. The moving average method and limiter has been used for the smooth waveform of the SOH observer. Very simple moving average filter was used. The purpose of the filter is to eliminate the chattering phenomena whose average value is zero. The equation for a filter is given as

$$Z_h = \frac{\hat{Z} + Z_h}{2}. \tag{44}$$

For every sampling time, the variables are updated using old variables.

The filtered SOC signal Z_h and the cell output voltage V_{ht} are fed into the SOH observer. The output signals are $\hat{Z}_h$, $\hat{C}_n$, and $\hat{R}_t$. The estimated parameters, viz., $\hat{C}_n$ and $\hat{R}_t$, also have chattering values. The moving average and limiter have been used for the smooth filtered signal. This signal is fed into the SOC observer for SOC estimation. The Euler backward method was used for the discrete-time equation.

The proposed sliding-mode observer was applied to the overall Urban dynamometer driving schedule (UDDS) cycle. The gains are listed in Table I. The resultant SOC for the whole UDDS cycle is shown in Fig. 8. The estimated SOC and the errors for all the UDDS cycles are shown in the Fig. 8. Due to the simple model, the SOC error can exceed 10% for a short period of time. However, in most of the time, the SOC error is bounded to 3%. The SOC error can be reduced if another RC network is added to the previous model. The trajectories are

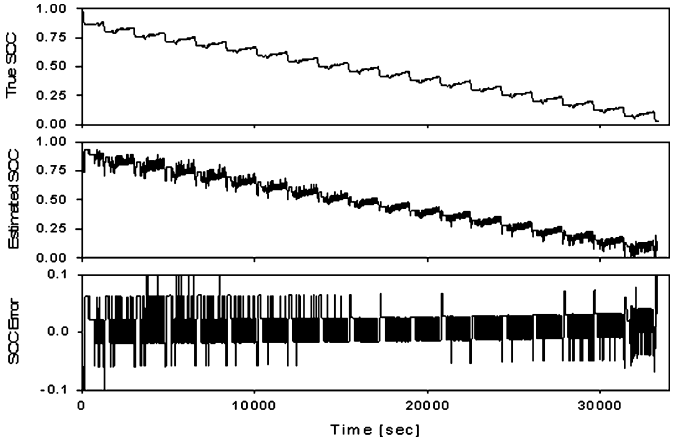

Fig. 8. Experimental result for the estimated SOC and error.

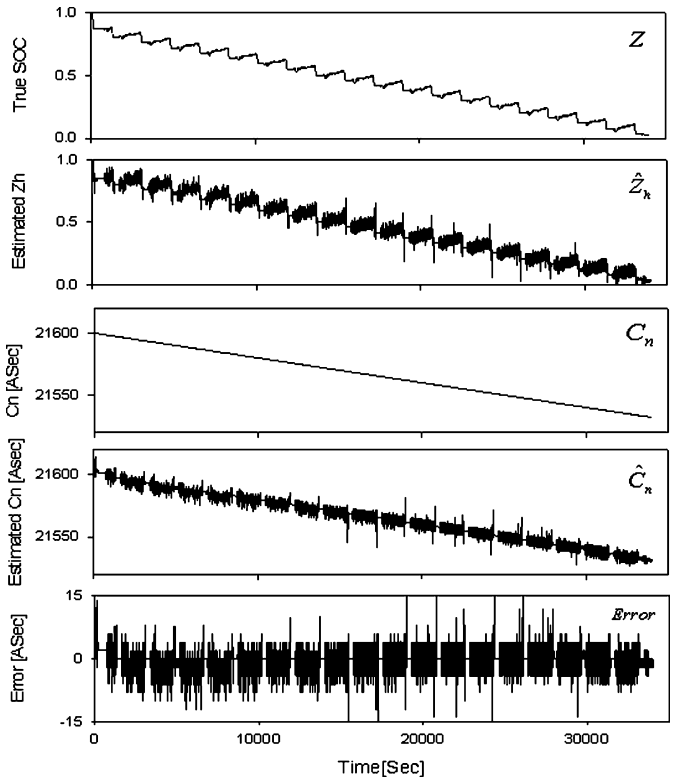

Fig. 9. Simulation result for the estimation of the capacity C_n.

always confined to the true SOC with the chattering value. This chattering can be smoothed by a saturation function instead of a sign function. In this way, the average value of the estimated SOC can be close to the true SOC. There can be seen the drifting bias in the SOC error. It is not zero mean. The drifting effect is due to the modeling errors. There exists a modeling error during the relaxation period, however, no error exists at the end of period, which corresponds to the OCV region. This is the reason for a drifting bias in the SOC error. It can be eliminated by adapting a more complicated model method. Therefore, the suggested sliding-mode observer can be directly applied to the real

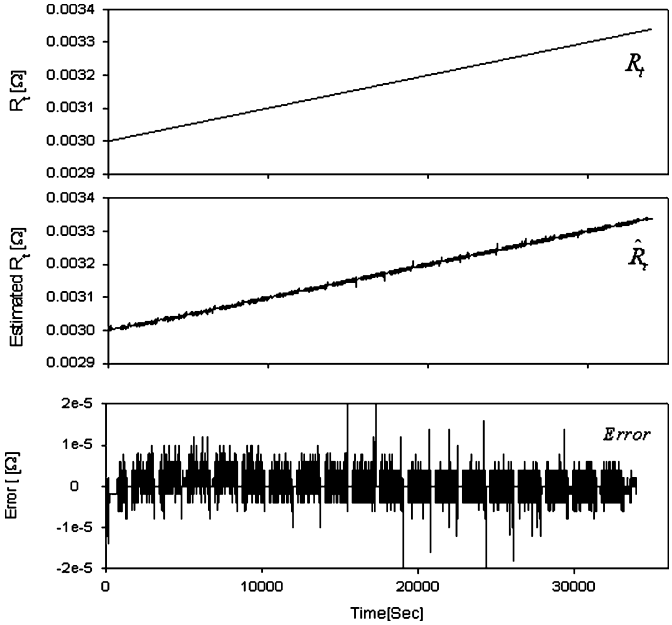

Fig. 10. Simulation result for the estimation of the resistance R_t.

driving environment of electric vehicles or HEVs for superior performance.

The simulation results for the capacity fade and resistance deterioration are shown in Figs. 9 and 10. As can be seen in Fig. 9, the estimated SOC $\hat{Z}_h$ is controlled to true SOC Z with a switching ripple. The estimated capacity $\hat{C}_n$ also follows the true C_n with a switching ripple. From Fig. 9, it can be seen that the designed sliding-mode observer is controlled to the switching surface, which is constructed from the error dynamics. The resistance can be estimated in a similar manner. Fig. 10 shows the result of resistance estimation. The result shows that the estimated resistance $\hat{R}_t$ follows R_t with a switching ripple. The proposed dual-sliding-mode observer can estimate the SOC and SOH with superior performance.

The true parameters for C_n and R_t are obtained from the accelerated life cycle test data. This cycle is composed of 5 A charge (1-C rate) and 72 A discharge (12-C rate). It may take 500 cycles to arrive at "half-life," typically 10% capacity degradation, or 50% resistance degradation. The result of life cycle test is shown in Fig. 11. It can be seen that the capacity has been increased during 100 cycles. It is thought that conductivity of the active material in the electrolyte has been increased during initial cycle period. The capacity has been decreased to 90% of initial value after 500 cycles. The result of the capacity-fade estimation using proposed observer are shown in Fig. 12. The initial value was set to 5800 A·h. The moving average filter was used in order to reduce the chattering in the estimated value. The details of the figures are little bit different, which is caused by the different test condition and nonlinear characteristics of the cell; however, the general figure profiles are similar. It can be seen that the proposed system shows excellent tracking performance.

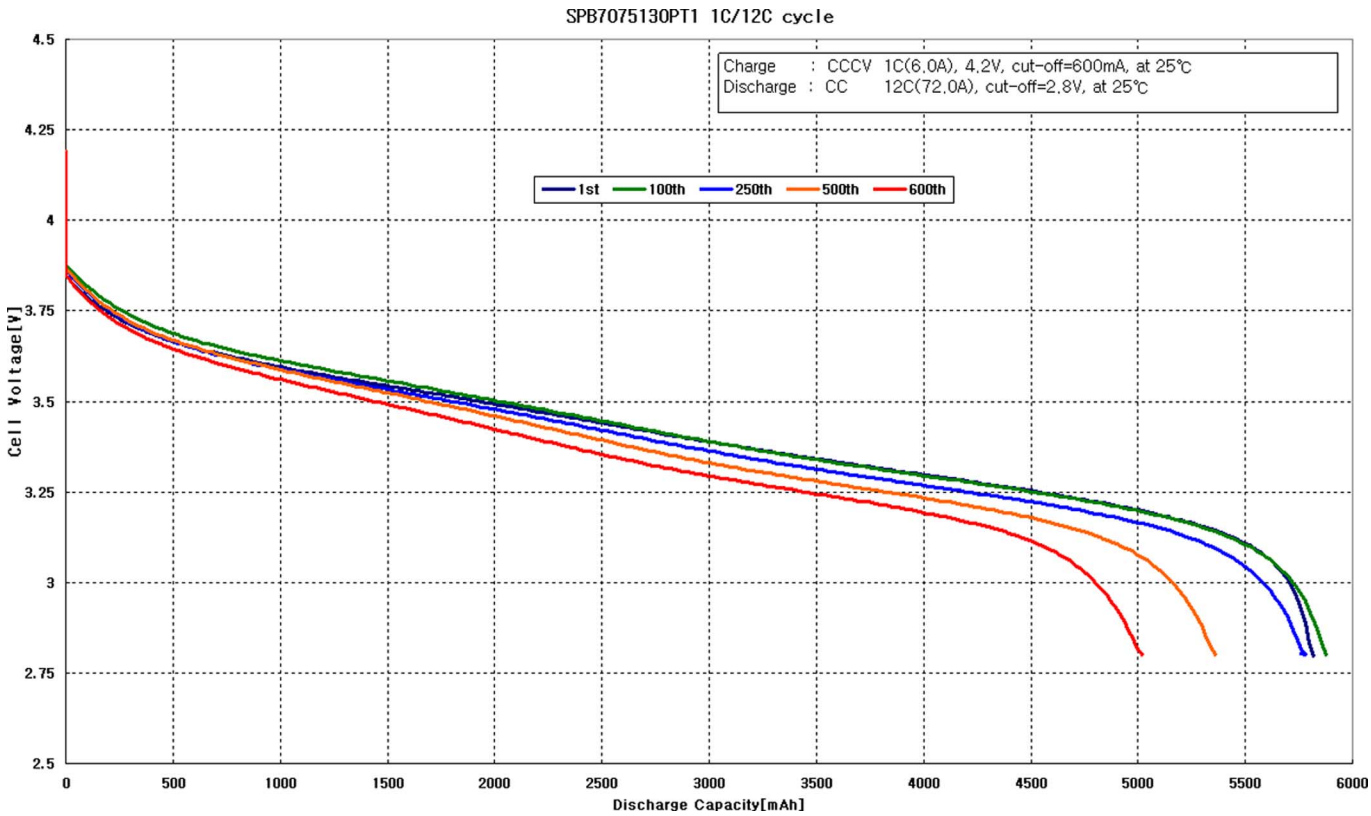

Fig. 11. Experimental result of life cycle test.

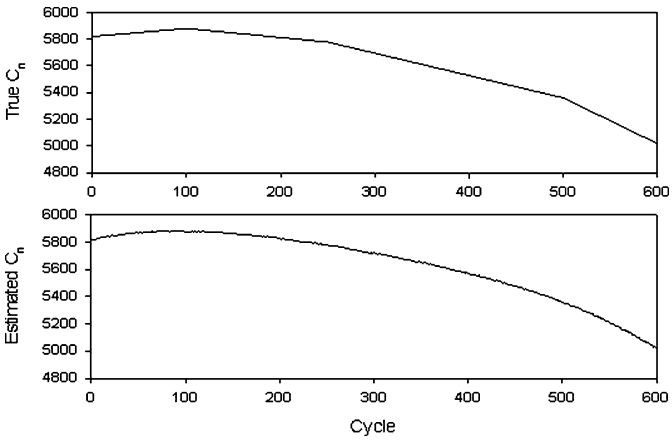

Fig. 12. Experimental result for capacity-fade estimation.

VII. Conclusion

A dual-sliding-mode-observer design method for estimating the SOC and SOH of Li-PB batteries has been presented in this paper. A simple RC model was used for Li-PB modeling and the errors or uncertainties in modeling that are caused by the simple model were compensated for by the proposed sliding-mode observer system. A systematic design method has been presented and the Lyapunov inequality equation has been invoked to establish the convergence of the proposed observer. The performance of the proposed system has been verified by a UDDS cycle test, which is a very harsh environmental test. The SOC error is confined to an acceptable level, i.e., less than 3% in most cases, which is adequate for real environments. The results on parametric estimation through the dual-sliding-mode observer show excellent tracking performance for the duration of cell degradation.

References

[1] M. Dubarry, N. Vuillaume, and B. Y. Liaw, "From single cell model to battery pack simulation for Li-ion batteries," *J. Power Sources*, vol. 186, pp. 500–507, 2009.

[2] R. Kaiser, "Optimized battery-management system to improve storage lifetime in renewable energy system," *J. Power Sources*, vol. 168, pp. 58–65, 2005.

[3] S. S. Williamson, S. C. Rimmalapudi, and A. Emadi, "Electrical modeling of renewable energy sources and energy storage devices," *J. Power Electron.*, vol. 4, no. 2, pp. 117–126, Apr. 2004.

[4] S. Brown, K. Ogawa *et al.*, "Cycle life evaluation of 3Ah LixMn2O4 base lithium-ion secondary cells for low-earth-orbit satellite," *J. Power Sources*, vol. 185, pp. 1444–1453, 2008.

[5] L. Maharjan, S. Inoue, H. Akagi, and J. Asakura, "State-of-Charge (SOC)-balancing control of a battery energy storage system based on a cascade PWM converter," *IEEE Trans. Power Electron.*, vol. 24, no. 6, pp. 1628–1636, Jun. 2009.

[6] V. Boovaragavan, S. Harinipriya, and V. R. Subramanian, "Towards real-time parameter estimation of lithium-ion batteries using reformulated physics-based model," *J. Power Sources*, vol. 183, pp. 361–365, 2008.

[7] S. H. Huh, S. J. Seo, I. Choy, and G. T. Park, "Design of a robust stable flux observer for induction motors," *J. Electr. Eng. Technol.*, vol. 2, no. 2, pp. 280–285, 2007.

[8] W. L. Burgess, "Valve regulated lead acid battery float service life estimation using a Kalman filter," *J. Power Sources*, vol. 191, no. 1, pp. 16–21, Jun. 2009.

[9] G. L. Plett, "Extended Kalman filtering for battery management system of LiPB-based HEV battery packs—Part 1, 2, 3," *J. Power Sources*, vol. 134, pp. 252–292, 2004.

[10] B. S. Bhangu, P. Bentley, and C. M. Bingham, "Nonlinear observers for predicting state-of-charge and state-of-health of lead-acid batteries for hybrid-electric vehicle," *IEEE Trans. Veh. Technol.*, vol. 54, no. 3, pp. 783–794, May 2005.
[11] F. Huet, "A review of impedance measurements for determination of the state-of-charge or state-of-health of secondary batteries," *J. Power Sources*, vol. 70, pp. 59–69, 1998.
[12] I. S. Kim, "Nonlinear state of charge estimator for hybrid electric vehicle battery," *IEEE Trans. Power Electron.*, vol. 23, no. 4, pp. 2027–2034, Jul. 2008.
[13] I. Park and S. Kim, "A sliding mode observer design for fuel cell electric vehicles," *J. Power Electron.*, vol. 6, no. 2, pp. 172–177, Apr. 2006.
[14] F. F. M. El-Sousy, "Robust tracking control based on intelligent sliding-mode model-following position controllers for PMSM servo drives," *J. Power Electron.*, vol. 7, no. 2, pp. 159–173, Apr. 2007.
[15] P. E. Pascoe and A. H. Anbuky, "VRLA battery discharge reserve time estimation," *IEEE Trans. Power Electron.*, vol. 19, no. 6, pp. 1515–1522, Nov. 2004.
[16] S.-C. Tan, Y. M. Lai, and C. K. Tse, "Indirect sliding mode control of power converters via double integral sliding surface," *IEEE Trans. Power Electron.*, vol. 23, no. 2, pp. 600–611, Mar. 2008.
[17] M. Gokasan, S. Bogosyan, and D. J. Goering, "Sliding mode based power-train control for efficiency improvement in series hybrid-electric vehicles," *IEEE Trans. Power Electron.*, vol. 21, no. 3, pp. 779–790, May 2006.
[18] W. Qiao, W. Zhou, J. M. Aller, and R. G. Harley, "Wind speed estimation based sensorless output maximization control for a wind turbine driving a DFIG," *IEEE Trans. Power Electron.*, vol. 23, no. 3, pp. 1156–1169, May 2008.

IL-Song Kim (M'04) was born in Korea, in 1968. He received the B.S. degree in electronics engineering from Yonsei University, Seoul, Korea, in 1991, the M.S. and Ph.D. degrees in electrical engineering from Korea Advanced Institute of Science and Technology (KAIST), Daejeon, Korea, in 1994 and 2005, respectively.

From 1994 to 1999, he was with the Satellite Business Division, Hyundai Electronics, Korea. From 1999 to 2003, he was a Power Team Leader at the Satellite Research Center in the KITSAT-4 satellite project, where he was engaged in designing the solar battery charger and manufactured battery pack. From 2005 to 2007, he was with Battery R&D, LG Chemical, where he was involved in the development of the battery management system of hybrid electric vehicle with Hyundai Motors. Since 2007, he has been an Assistant Professor in the Department of Electrical Engineering, Chung-Ju National University, Chungju, Korea. His current research interests include photovoltaic system, satellite power and system engineering, aerospace electronic equipment, and control systems. He was registered in the Marquis Who's Who in Science and Engineering and International Biographical Centre in 2000 outstanding scientists.